A general photocatalytic strategy for nucleophilic amination of primary and secondary benzylic C–H bonds

Madeline E. Ruos,[‡a] R. Garrison Kinney,[‡†ab] Oliver T. Ring,[ac] and Abigail G. Doyle[*a]

[a]Department of Chemistry and Biochemistry, University of California-Los Angeles, Los Angeles, CA, 90095, USA; [b]Department of Chemistry, Princeton University, Princeton, NJ 08544, USA.; [c]Early Chemical Development, Pharmaceutical Sciences, Biopharmaceuticals R&D, AstraZeneca Gothenburg, SE-431 83 Mölndal, Sweden.

KEYWORDS C(sp³)–H activation, photoredox catalysis, radical-polar crossover

ABSTRACT: We report a visible-light photoredox-catalyzed method that enables nucleophilic amination of primary and secondary benzylic C(sp^3)–H bonds. A novel amidyl radical precursor and organic photocatalyst operate in tandem to transform primary and secondary benzylic C(sp^3)–H bonds into carbocations via sequential hydrogen atom transfer (HAT) and oxidative radical-polar crossover (ORPC). The resulting carbocation can be intercepted by a variety of *N*-centered nucleophiles, including nitriles (Ritter reaction), amides, carbamates, sulfonamides, and azoles for the construction of pharmaceutically-relevant C(sp^3)–N bonds under unified reaction conditions. Mechanistic studies indicate that HAT is amidyl radical-mediated and that the photocatalyst operates via a reductive quenching pathway. These findings establish a mild, metal-free, and modular protocol for the rapid diversification of C(sp^3)–H bonds to a library of aminated products.

INTRODUCTION

The merger of hydrogen atom transfer (HAT) with transition metal-catalyzed oxidative radical relay (ORR) or oxidative radical polar crossover (ORPC) has recently emerged as a promising strategy to enable mild C(sp^3)–H functionalization reactions with nucleophilic coupling partners.[1] Due to the prevalence of nitrogen functionality in bioactive compounds, this strategy is of particular interest as an approach to C(sp^3)–H amination for feedstock chemical conversion and late-stage derivatization.[2] C(sp^3)–H amidations proceeding via HAT-ORPC (Ritter-type reactions) have been reported under a variety of oxidative conditions using solvent quantities of nitrile as the nucleophile.[3] Of note, Lambert and coworkers have reported a mild method for Ritter-type C–H amidation via electrophotocatalysis, the only example to date that does not require stoichiometric oxidant.[4] Whereas most Ritter reactions target secondary and tertiary benzylic or unactivated tertiary C(sp^3)–H bonds, recently König and coworkers have disclosed a unique strategy for Ritter amidation, utilizing visible light excitation of *in situ*-generated iodine(III)-BF_3 complexes to amidate primary benzylic C–H bonds.[5]

Despite these important advances, expansion of *N*-nucleophile identity beyond nitriles in solvent quantity is comparatively less explored. Copper-catalyzed platforms, including variants of the original Karasch-Sosnocky reaction[6] as well as more recent developments by Stahl, Liu, and others have proven most versatile, enabling C–H (sulfonyl)amidation,[7–13] azolation,[14] and azidation.[15,16] Alternatively, transition metal-free platforms for C(sp^3)–H (sulfonyl)amidation[17–19] and C(sp^3)–H azolation[20–23] exist, but each method and reaction conditions is confined to a single nucleophile class (amides, sulfonamides, or azoles, but never all three within one protocol). Moreover, many still require stoichiometric strong oxidants such as Selectfluor, NFSI, or DDQ, which limit the scope of the methods. Thus, identification of reagents and catalysts that can enable selective activation of a wider array of C(sp^3)–H partners, under more practical and functional group-tolerant conditions, and with greater generality with respect to NH-nucleophile identity would be of broad value.

With this in mind, we questioned whether recent work in our lab,[24] reported concurrently with the Musacchio lab,[25] combining HAT with photocatalytic oxidative radical-polar crossover (HAT-ORPC) might be suited to the development of a general and mild C(sp^3)–H amination. Our prior reaction platform included Ir(*p*-F-ppy)$_3$ as a photocatalyst and *N*-acyloxyphthalimide as the HAT precursor and we demonstrated that this platform enabled fluorination of secondary and tertiary benzylic and allylic C(sp^3)–H bonds (Figure 1C). Whereas other nucleophiles such as chloride, alcohols, thiols, and water were also tolerated, nitrogen-based nucleophiles were unreactive aside from a single report of C(sp^3)–H azidation. Likewise, Musacchio and coworkers reported only a single example of C–N bond formation using a pyrazole derivative;[25] they have since expanded this catalyst platform to include secondary benzylic and tertiary benzylic and aliphatic C(sp^3)–H azolations.[23]

In our original report, inclusion of NEt_3•3HF was necessary in order to obtain high yields of C(sp^3)–H functionalization (even for non-fluoride nucleophiles), likely because this additive accelerated single-electron reduction and decarboxylation of *N*-acyloxyphthalimide with excited-state Ir(*p*-F-ppy)$_3$, affording higher concentrations of the HAT reagent (methyl radical). However, we found that NH-nucleophiles such as sulfonamides and amides were deactivated by competitive hydrogen bonding with the NEt_3•3HF additive. Hydrogen bonding to the NH-nucleophile also inhibited methyl radical generation from *N*-acyloxyphthalimide, NEt_3•3HF and Ir(*p*-F-ppy)$_3$. We hypothesized that identification of novel HAT precursors that deliver polarity-matched HAT agents under less reducing

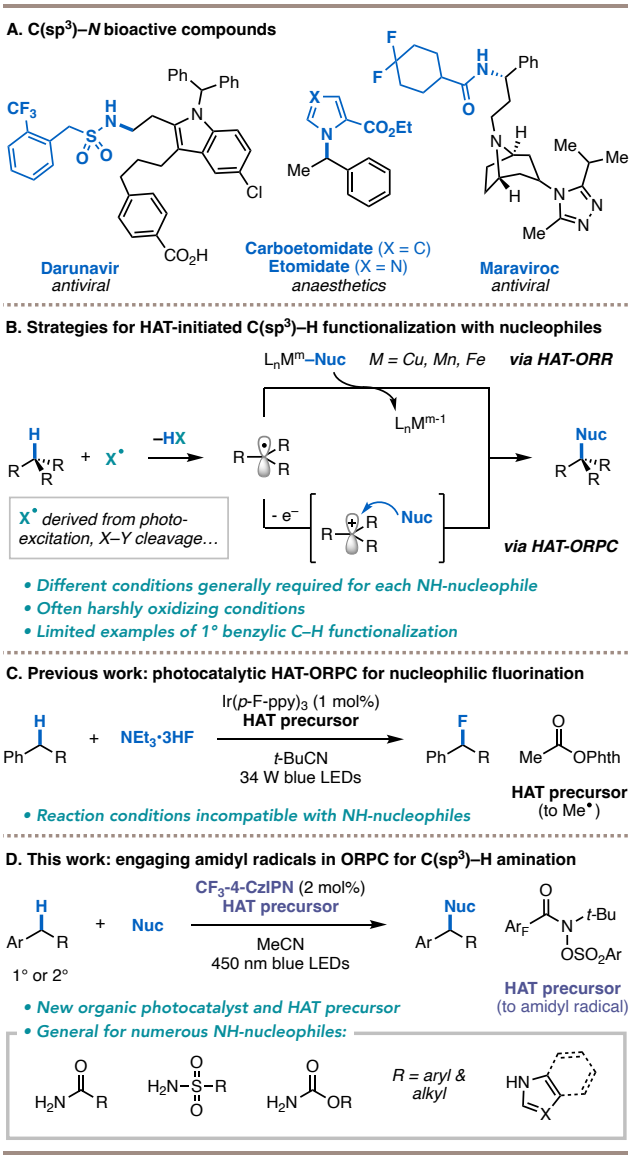

Figure 1. Prior art in C(sp^3)–H functionalization with *N*-nucleophiles and overview of this work.

conditions and/or a photoredox catalyst with an expanded redox window for reductive generation of the HAT reagent and radical oxidation could address this limitation.

We describe below the application of a novel amidyl radical HAT precursor and new organic photoredox catalyst to a mild, Ritter-type C(sp^3)–H amidation with acetonitrile and water, and amination with a range of exogenous N-nucleophiles such as amides, sulfonamides, carbamates, and azoles (Fig. 1D). Moreover, we establish the versatility of this platform to achieve C(sp^3)–H halogenation, esterification, etherification, and hydroxylation. Data science-informed evaluation of the C(sp^3)–H substrate scope reveals the breadth and limitations of this method for secondary benzylic C(sp^3)–H substrates. Notably, primary benzylic C(sp^3)–H sites of abundant toluene-derived feedstocks also undergo amidation. Finally, in-depth mechanistic studies are presented which show reductive quenching of the photocatalyst by the HAT reagent enables the HAT-ORPC catalytic cycle to take place.

RESULTS AND DISCUSSION

Our optimization studies began with the preparation and evaluation of a series of new HAT precursors. Amidyl radicals containing 3,5-bis(trifluoromethyl) substitution on the benzamide moiety, along with *tert*-butyl substitution on nitrogen were targeted as HAT agents on the basis of precedent from the Alexanian group who has demonstrated that this motif is highly effective in engaging in rapid and selective intermolecular hydrogen atom abstraction.[26] Photocatalytic reductive generation of amidyl radicals has been previously achieved using *O*-aryl,[27] *O*-benzoyl,[28] and very recently *O*-alkenyl[29,30] hydroxamic acid derivatives. Nevertheless, implementation of these reagents in an ORPC platform is currently unknown and presents multiple challenges. In particular, the propensity for charge recombination after single-electron reduction could result in extremely small concentrations of all down-stream species, rendering HAT and radical oxidation kinetically slow.[31,32] We reasoned that installation of a sulfonate ester leaving group on the nitrogen center would address this requirement and a few others:[33] (1) it would provide a strong thermodynamic driving force for single-electron reduction; (2) facilitate selective mesolytic fragmentation, (3) produce a sulfonate anion that would not interfere with nucleophilic trapping, and (4) confer stability under blue light irradiation. Similar *N*-sulfonate (sulfon)amides have been previously reported as precursors to sulfonamidyl radicals that undergo addition to electron-rich heterocycles.[34,35] HAT reagents **A–C** were prepared in two steps without chromatography, giving bench-stable solids (Figure 2).

We interrogated these HAT reagents in a Ritter-type C(sp^3)–H amidation of ethylbenzene (**1a)** to afford acetamide **1b** using acetonitrile as the solvent and H_2O (2 equiv) as a nucleophile (Figure 2). Employing HAT reagent **A** (1 equiv) afforded product **1b** in 69% yield using Ir(*p*-F-ppy)$_3$ as a photocatalyst (entry **1**). Analysis of the ^{19}F NMR spectrum of the crude reaction mixture revealed decomposition of the iridium photocatalyst and incomplete conversion of the HAT reagent. We thus turned our attention to the use of organic photocatalysts, in particular cyanoarene-based 4-CzIPN derivatives, which have demonstrated improved stability relative to transition metal photocatalysts in various photocatalytic transformations and represent more sustainable and cost-effective options.[36,37] Additionally, the modular features of organic CzIPN derivatives enables the systematic fine-tuning of both the donor substituents and acceptor core of the catalyst structure, which can expand the "redox window" of the photocatalysts. This makes them a more attractive platform for the development of radical-polar crossover reactions.[36] To our surprise, preliminary photocatalyst screening using high-throughput experimentation demonstrated many organic photocatalyst scaffolds were competent in the reaction (see Supporting Information). Although yields were lower when using 4-CzIPN and *t*-Bu-4-CzIPN (entries **3** and **4**) than Ir, no decomposition of the organic photocatalysts was observed at the end of the reaction.

When using the more oxidizing CF_3-4-CzIPN as a catalyst, a marked improvement in reactivity was observed, giving product **1b** in 80% yield (entry **2**). Such an improvement in yield may reflect CF_3-4-CzIPN's enhanced photophysical properties relative to 4-CzIPN, including higher photoluminescence quantum yield (PLQY), longer excited state lifetimes, and higher excited state energies.[38] While CF_3-4-CzIPN has been previously used in the development of thermally activated delayed fluorescence organic light-emitting diodes (TADF OLEDs),[38] to the best of our knowledge, it has not been used as a photocatalyst in a synthetic organic transformation.

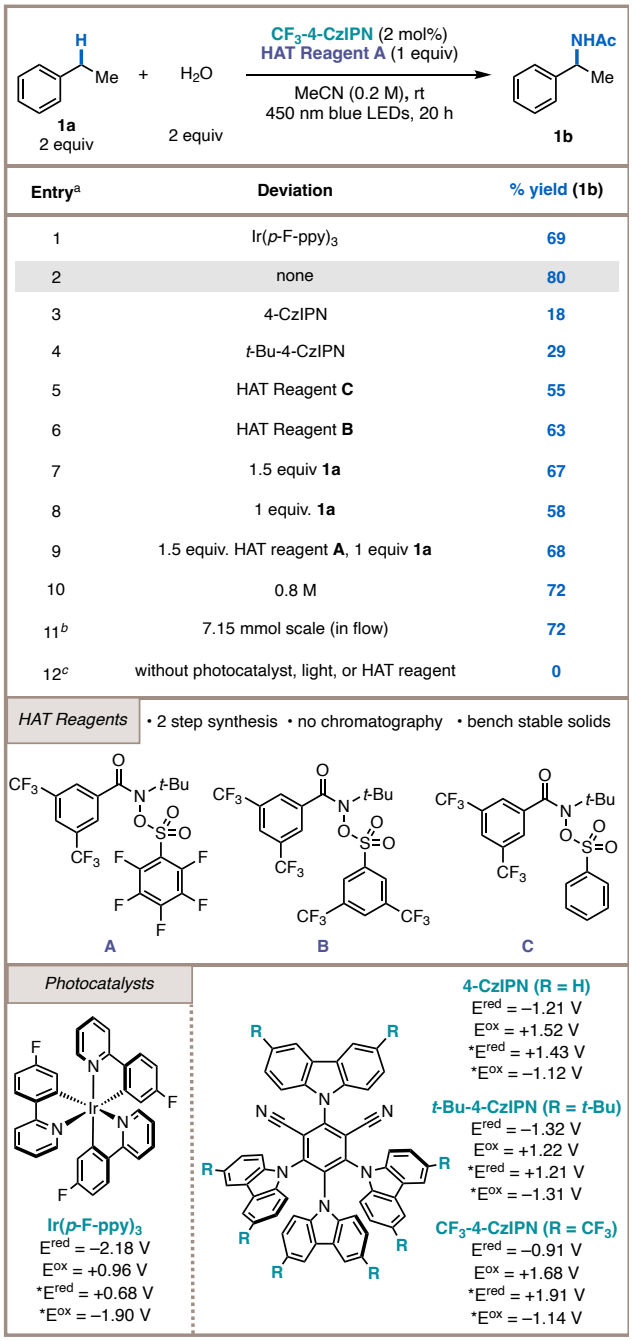

Figure 2. Optimization of reaction conditions. [a]Reactions run at 0.1 mmol scale. Yields determined by ^{1}H NMR spectroscopy with 1,3,5-trimethozybenzene as an external standard. Redox potentials are reported in volts vs SCE in MeCN. [b]For the exact reaction setup, see Supporting Information. [c]Reaction was performed independently without blue LEDs, without photocata-

Using CF_3-4-CzIPN as photocatalyst, Ritter amidation proceeds in poorer efficiency with HAT reagents **C** and **B** as compared to **A** (entries 5 and 6). The highly electron-withdrawing perfluoroarene on **A** likely leads to acceleration of both single-electron reduction by the photocatalyst and fragmentation to the amidyl radical. While 2 equivalents of C–H partner delivered optimal yields, using 1.5 or 1 equivalents of C–H partner instead still yields **1b** in 67% and 58% yield, respectively (entries **7** and **8**). Additionally, using 1 equivalent of **1a** with slight excess of HAT reagent **A** led to formation of acetamide **1b** in 68% yield (entry **9**). Repeating the reaction at higher concentrations (0.8 M) gives the desired product in slightly lower yield, likely due to the sparing solubility of the photocatalyst in acetonitrile (entry **10**). To highlight the practical utility of the conditions, the transformation was also conducted on a 7.15 mmol scale using an R-Series Vapourtec photoflow reactor setup which afforded the desired product in 72% yield (entry **11**, see Supporting Information for details on experimental setup). Finally, control experiments reveal that all components of the reaction are necessary to generate the product (entry **12**). Additional details of further optimization experiments, including for reactions with other nucleophiles and Ritter-type amidation of primary benzylic C–H substrates, are provided in the Supporting Information. These conditions represent an exceptionally mild method for performing Ritter-type amidation on benzylic C–H bonds relative to classical methods, which previously have relied on strong stoichiometric oxidants, high temperatures, and extended reaction times.

With optimized conditions in hand, we next turned our attention to the generality of the method. In an effort to systematically select a diverse collection of C–H substrates, we applied a data science-driven approach previously published by our group.[39] First, we searched the Reaxys® database for compounds containing a secondary benzylic C–H site which provided >3,000,000 compounds. This library was subsequently filtered based on molecular weight, commercial availability, available spectral data, and functional group compatibility (see Supporting Information for full details). Filtering in this manner provided a dataset of ~2500 substrates. To visualize this dataset, we next pursued molecular featurization using DFT to extract global (such as dipole, highest occupied molecular orbital energy, and electronegativity) and atomic features (such as buried volume and NMR shift) of the substrates. This was performed using Auto-QChem, a tool previously built by our group which automates the generation and storage of chemical descriptors for organic molecules in a web-accessible database.[40,41]

With the molecular featurization completed, we used Uniform Manifold Approximation and Projection (UMAP) to reduce the featurization to two dimensions for chemical space visualization.[42] To cover chemical space, we selected 45 molecules to evaluate under the optimized C(sp^3)–H amidation conditions. The Ritter amidation yields as determined by ^{1}H NMR of the crude reaction mixture and their distribution over the substrate chemical space are illustrated in Figure 3. Given the observed distribution of yields, we note that the method is relatively high yielding with a variety of compounds, particularly substrates in the upper left, right, and lower boundaries of the map (Fig. 3). Further reaction development will likely be required to identify conditions that enable C–H functionalization of substrates in the middle of the map, which performed poorly. Many of these substrates possess benzylic C–H bonds adjacent to a carbonyl derivative, making them less likely to engage in HAT with the electrophilic amidyl radical based on a polarity-mismatch. Additionally, these substrates tended to contain nitro groups *para* to the benzylic C–H bond, which presumably leads to strong deactivation towards HAT. The structures and associated ^{1}H NMR yields for all examples shown in Figure 3 can be found in the Supporting Information.

The substrates that delivered ^{1}H NMR yields > 30% were subjected to the Ritter conditions on 0.3-mmol scale to obtain isolated yields, as shown in Figure 3. We were pleased to find

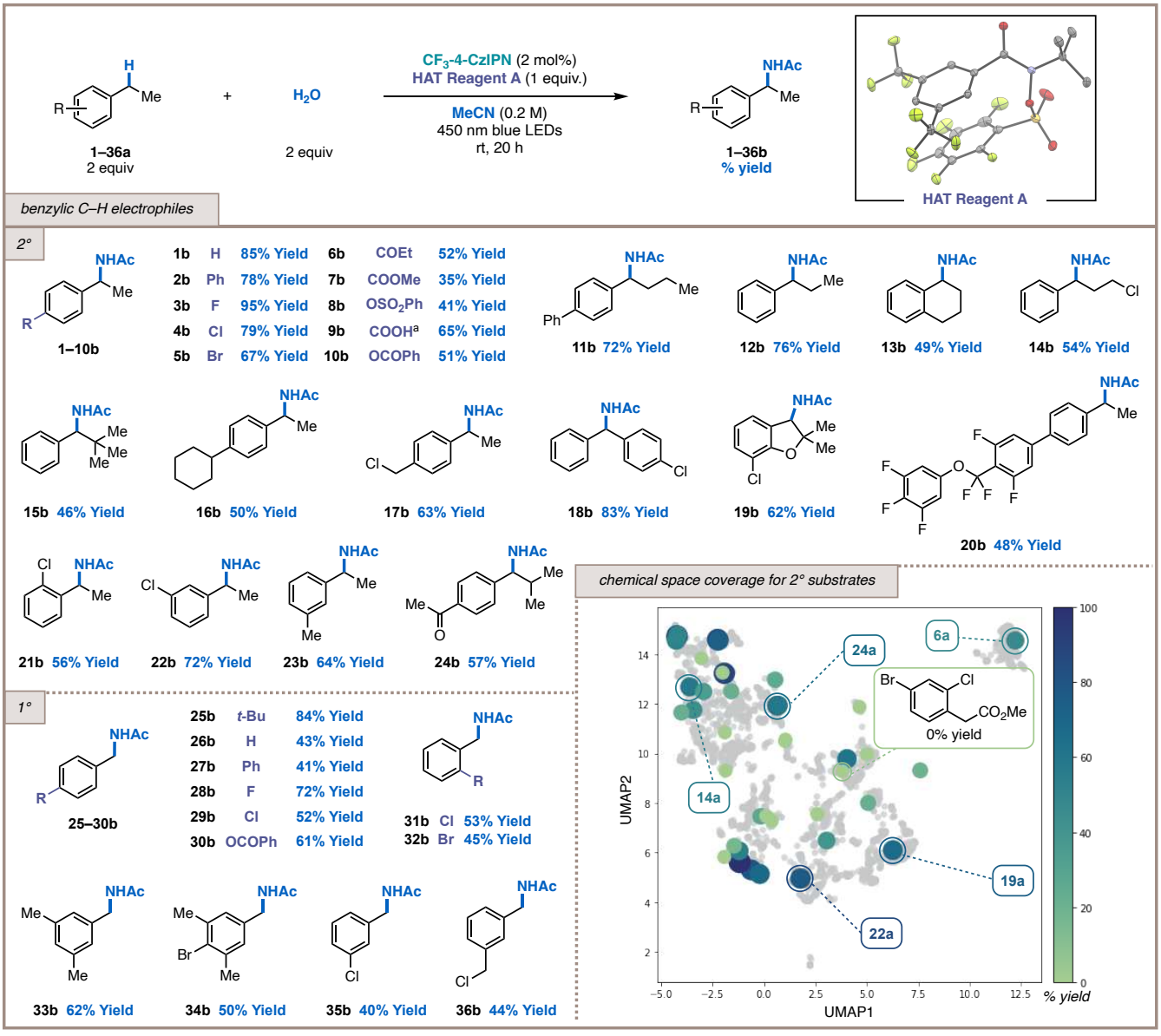

Figure 3. Substrate scope of benzylic C–H partners for photocatalytic Ritter amidation (0.3 mmol scale, isolated yields). For chemical space coverage, reactions were run on 0.1 mmol scale, and yields were determined by ^{1}H NMR spectroscopy with 1,3,5-trimethoxybenzene as an external standard. [a]Reaction performed on 0.1 mmol scale with 1,3,5-trimethoxybenzene added as an external standard (^{1}H NMR yield is reported).

that ethylbenzenes bearing a range of electronically diverse substituents were tolerated in the reaction, affording good to high yields of benzylic acetamide products (**1–10b**). Potentially reactive functional groups such as esters (**7b**), carboxylic acids (**9b**), phenol derivatives (**8b, 10b**), benzylic halides (**17b**), and aryl halides (**3–5b, 19–22b**) were all tolerated in the reaction. Various cyclic and acyclic *n*-alkyl benzenes (**11–15b**) underwent selective amidation at the benzylic site. For substrates that contained multiple benzylic C–H bonds (**16–18b, 23b**), we observed exclusive regioselectivity for functionalization at the secondary benzylic C–H site. Of note, despite two secondary benzylic C–H sites in substrates **17a**, we observe complete selectivity for abstraction of the more hydridic C–H bond. Finally, substrates with greater structural complexity (**19b, 20b**) were suitable coupling partners.

The abundance and affordability of toluenes led us to examine their use as substrates for the photocatalytic amidation. We found that a variety of *para*-substituted toluene derivatives **25–30a** underwent reaction in 41–84% yield when the photocatalyst loading was increased to 5 mol%. Additionally, *meta*- and *ortho*-substituted toluenes **31–36a** were successful in the reaction. Noteworthy amongst these examples, benzylic halide **36a** gives the corresponding acetamide product with exclusive selectivity for the primary C–H position while leaving the benzylic chloride and 2° C–H's intact. Moreover, no difunctionalization is observed for both primary and secondary C–H substrates, a testament to the mildness of the reaction conditions and selectivity via polarity matching with the amidyl radical HAT reagent. Overall, these results represent a relatively rare example of Ritter C(sp^3)–H amidation that operates on primary benzylic substrates, serving as a complement to alternative protocols that operate on tertiary and secondary substrates exclusively.

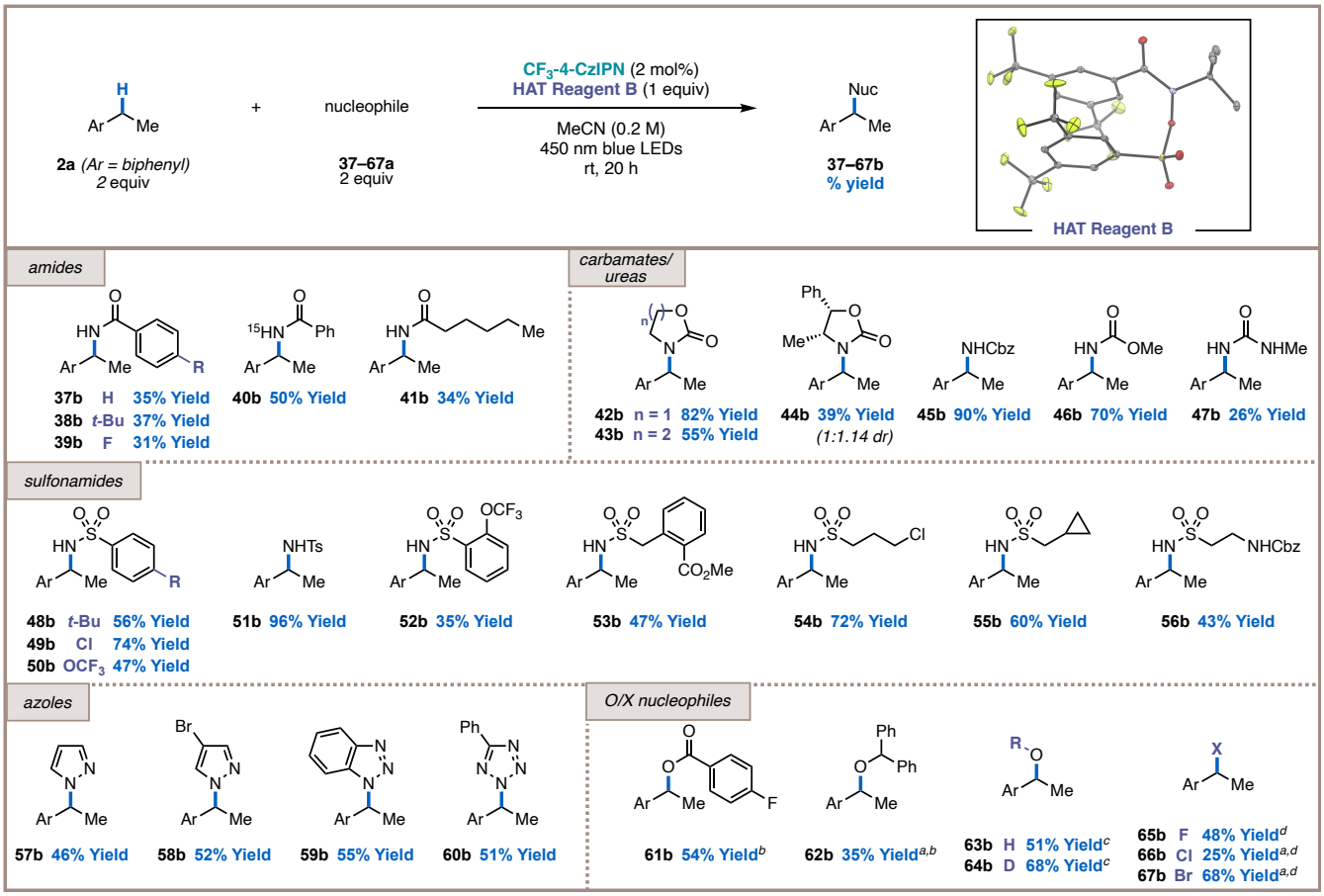

Figure 4. Substrate scope of nucleophiles for photocatalytic C(sp^3)–H functionalizations (0.3 mmol scale, isolated yields). [a]Reactions performed on 0.1 mmol scale with 1,3,5-trimethoxybenzene added as an external standard (^{1}H NMR yield is reported, average of 2 runs) [b]Reactions performed with 1.5 equiv. 2,4,6-tri-tert-butylpyridine. [c]Reactions performed with 2 mol% of *t*-Bu-4-CzIPN as photocatalyst, 28 equiv. of nucleophile, and 1 equiv. of K_3PO_4. [d]Reactions performed with 6 equiv. of nucleophile (65b: NEt_3•3HF; 66b: TBACl; 67b: TBABr)

We next sought to evaluate whether this strategy could serve as a more general blueprint for C(sp^3)–H amination with amides, carbamates, ureas, sulfonamides, and azoles, all of which are important motifs in pharmaceutically relevant bioactive compounds. Indeed, replacement of water with 2 equiv of an *N*-nucleophile under the optimized Ritter conditions and switching to HAT reagent **B** afforded C(sp^3)–H (sulfonyl)amidation with both aliphatic and aromatic primary amides (**37–41b**) and sulfonamides (**48–56b**) in 31–96% yield. Of particular importance, installing aliphatic amides and sulfonamides proceeds efficiently, with yields up to 72%. Functionalization with [^{15}N]-benzamide afforded product in 50% yield, providing a simple route for the generation of ^{15}N-labeled compounds in two steps starting from inexpensive and commercially-available [^{15}N]-NH_4Cl. Cyclic and acyclic carbamates were readily coupled (**42–46b**), offering a potentially valuable avenue to introduce protected amine functionality in a synthetic sequence. Using a chiral oxazolidinone as a nucleophile delivered product **44b** in 39% yield as a 1:1.14 diastereomeric ratio at the newly formed stereocenter. Additionally, we found that C–N bond construction was possible from a variety of electron-rich nitrogen heterocycles. Couplings with pyrazoles (**57b**, **58b**, 46–52% yield), triazole (**59b**, 55% yield), and tetrazole (**60b**, 51% yield) motifs all resulted in good yields of the desired product.

Although not the main focus of our study, these conditions also translated to the incorporation of alternative nucleophiles such as halides (**65b–67b**), including bromination and fluorination in 68% and 48% yield, respectively. Additionally, ureas (**47b**), carboxylic acids (**61b**), alcohols (**62b**), and water (**63b, 64b**) are all compatible nucleophiles, highlighting the generality of this platform for C(sp^3)–H functionalization beyond simply Ritter-type amidation. This approach is potentially attractive from a medicinal chemistry perspective, where a single set of reaction conditions can rapidly generate a diverse library of C–H functionalized products.

The breadth of compatible nucleophiles for this transformation, along with the effectiveness of the new trifluoromethylated photocatalyst, prompted us to interrogate the mechanistic features of this reaction. Our initial hypothesis was that an amidyl radical was being generated *in situ* from HAT reagent **A** via an oxidative photocatalytic quenching cycle, similar to the mechanism proposed in our prior work on HAT-ORPC fluorination.[24] In this cycle, excited-state CF_3-4-CzIPN performs a single-electron reduction of the HAT reagent, inducing mesolytic cleavage. From there, the oxidized photocatalyst would be responsible for oxidizing the benzylic radical formed after HAT, completing the ORPC.

Based on this mechanistic rationale, we first sought to confirm the generation of *N-tert*-butyl radicals in the reaction. Indeed, *N-tert*-butylamide **68** was isolated from a typical reaction mixture in high yield (Fig. 5A). Furthermore, when the benzylic C(sp^3)–H partner and nucleophile were replaced by 1,1-

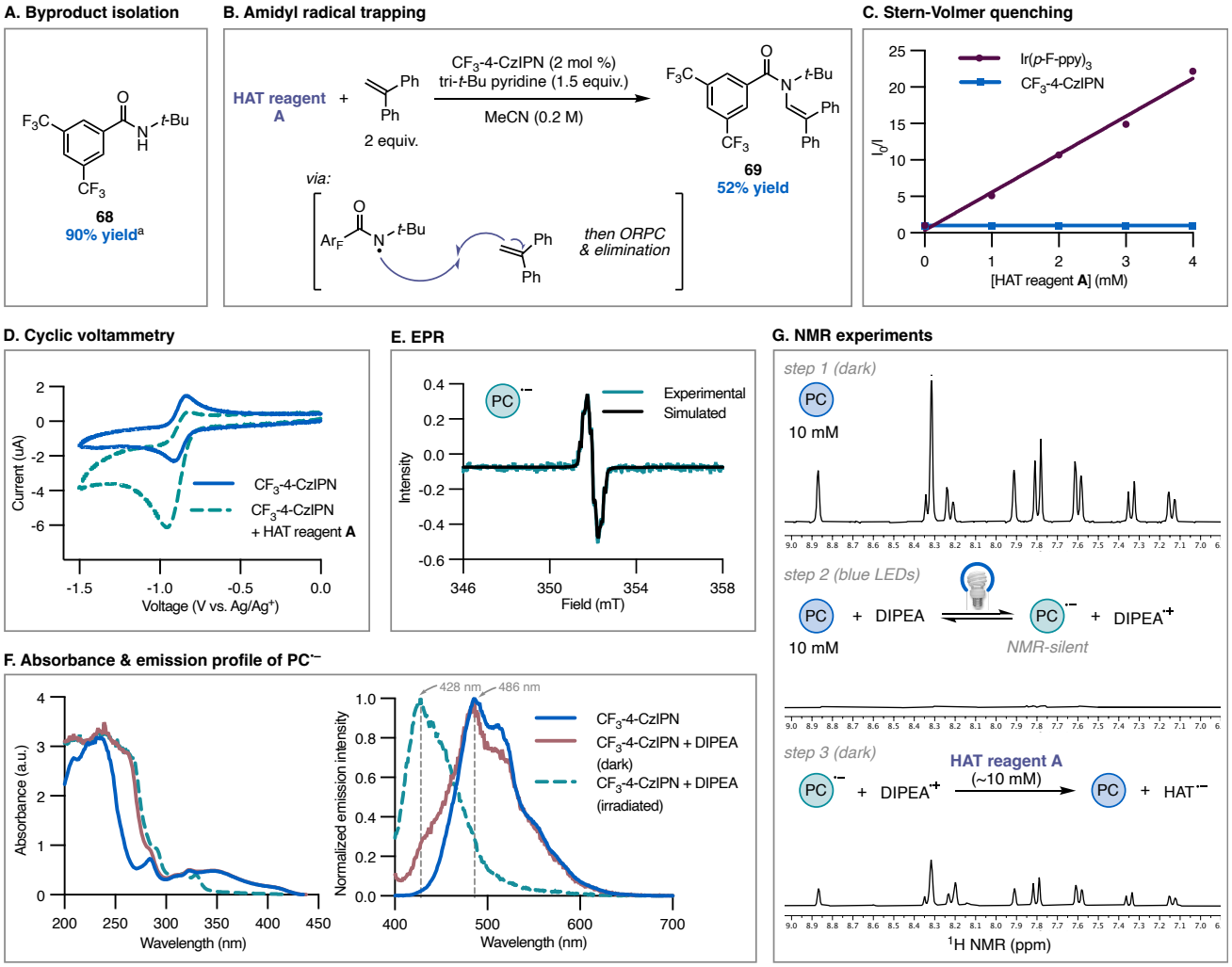

Figure 5. Mechanistic experiments supporting proposed mechanism. (A) Isolation of HAT reagent **A** byproduct under the standard reaction conditions shown in Fig. 3. (B) Amidyl radical trapping experiment with HAT reagent **A**. (C) Stern-Volmer luminescence quenching experiments (excitation at 395 nm). (D) Cyclic voltammograms of CF_3-4-CzIPN with and without added HAT reagent **A**. (E) Experimental and simulated EPR spectra to support the presence of CF_3-4-CzIPN$^{\bullet-}$. (F) Absorbance and emission profiles for CF_3-4-CzIPN and CF_3-4-CzIPN$^{\bullet-}$ (1.0 mM, 1.0 cm path length, excitation at 390 nm). (G) NMR spectroscopic evidence supporting the proposed reductive quenching cycle.

diphenylethylene, the enamide **69** was obtained, arising from addition of the nitrogen-centered radical into the alkene, followed by oxidation and base-mediated elimination (Fig. 5B). With evidence that HAT reagent **A** affords amidyl radical under the reaction conditions, we next sought to probe the mechanism by which the amidyl radical is generated. First, we carried out a series of Stern-Volmer luminescence quenching experiments (Fig. 5C).

To our surprise, HAT reagent **A** does not quench the luminescence of CF_3-4-CzIPN, indicating the reaction is unlikely to proceed via oxidative quenching with this photocatalyst. Additional experiments revealed that none of the reaction components quenched the excited-state CF_3-4-CzIPN photocatalyst (see Supporting Information), including ethylbenzene, ruling out direct oxidation of the C(sp^3)–H substrate. UV–Vis spectroscopy experiments demonstrated that an electron-donor-acceptor (EDA) complex between HAT reagent **A** and CF_3-4-CzIPN is also unlikely to facilitate single-electron redox chemistry (see Supporting Information). However, Stern-Volmer experiments do indicate that **A** efficiently quenches the excited-state of Ir(*p*-F-ppy)$_3$ (Fig. 5C). This suggests divergent mechanisms, indicative that product formation with more reducing photocatalysts such as Ir(*p*-F-ppy)$_3$ is occurring via an oxidative quenching pathway, while the more oxidizing CF_3-4-CzIPN is not sufficiently reducing in the excited-state to enable HAT reagent activation in this way.

From these data, we considered alternative potential mechanisms. The quantum yield of this transformation was measured to be 0.002, indicating that a radical chain process is unlikely or inefficient, and that the reaction is most likely unimolecular with respect to the photocatalyst.[43] Instead, we questioned whether a reductive quenching cycle could be operative, wherein the radical anion of CF_3-4-CzIPN is responsible for single-electron reduction of the HAT reagent. Cyclic voltammograms revealed that the reduction potential of HAT reagent **A** is –1.36 V vs SCE, making reduction of **A** by the CF_3-4-CzIPN radical anion thermodynamically uphill by ~ 9 kcal/mol. Nonetheless, given the slightly elevated reaction temperature in the

photoreactors and subsequent irreversible, exergonic steps following single-electron reduction, this step could be feasible. To determine whether this elementary step was operable, we carried out voltammetry on solutions containing CF_3-4-CzIPN and HAT reagent **A** (Fig. 5D). While voltammograms of the photocatalyst alone were reversible, when both species were present, an increased current response and lack of reversibility for the PC/PC$^{\bullet-}$ couple was observed.[44] These results suggest that reduction of HAT reagent **A** is likely occurring via an SET mechanism mediated by the radical anion of CF_3-4-CzIPN, consistent with our earlier results from Stern-Volmer luminescence quenching experiments.

To gain more insight into this mechanistic possibility, various spectroscopic studies and control experiments were performed. First, upon irradiation of a solution of CF_3-4-CzIPN and DIPEA with blue LEDs, a color change from light yellow to dark yellow/orange was observed. UV–Vis spectroscopy demonstrated a blue-shift of the maximum absorption peak (Fig. 5F, left). Upon irradiation of these two species, normalized emission spectra reveal a hypsochromic shift (from 486 nm to 428 nm), indicating the formation of a new species, analogous to previously-published results for 4-CzIPN (Fig. 5F, right).[45] To verify that this new species is indeed the radical anion CF_3-4-CzIPN$^{\bullet-}$, electron paramagnetic resonance (EPR) spectroscopy was performed (Fig. 5E). The experimental and simulated EPR spectra for CF_3-4-CzIPN$^{\bullet-}$ are in agreement, lending support for the formation of this reduced photocatalytic intermediate.

To obtain direct evidence of the ability of PC$^{\bullet-}$ to reduce HAT reagent **A**, we turned to ^{1}H NMR experimentation. The characteristic NMR signals of CF_3-4-CzIPN were detected from a mixture of the photocatalyst and DIPEA in CD_3CN in a J. Young NMR tube (Fig. 5G, step 1). Upon direct exposure of the solution within the NMR tube to 450 nm blue LEDs for 5 minutes (Fig. 5G, step 2), we observe line broadening and significant signal reduction, most likely due to the generation of a paramagnetic CF_3-4-CzIPN$^{\bullet-}$ species, which has a strong influence on NMR resonance relaxation rates due to the presence of an unpaired electron. Under nitrogen, this species was stable for at least 2 hours and could be quenched by exposure of the NMR tube to air to convert the photocatalyst back to the ground state. Upon addition of HAT reagent **A** to the radical anion species in the absence of light, a similar quenching effect was observed. We observed NMR signals consistent with reformation of the ground-state CF_3-4-CzIPN photocatalyst (Fig. 5G, step 3). Additionally, when HAT reagent **A** is added to an EPR sample of CF_3-4-CzIPN$^{\bullet-}$, a loss of signal is observed, indicative that the paramagnetic radical anionic species no longer exists (see Supporting Information). This is consistent with a proposal that the radical anion CF_3-4-CzIPN$^{\bullet-}$ reduces the HAT reagent, prompting fragmentation to its reactive amidyl radical species which then subsequently engages in HAT.

While the NMR experiments described are suggestive that the ground-state PC$^{\bullet-}$ is reducing HAT reagent, under the standard reaction conditions, which include constant irradiation with blue LEDs, we cannot necessarily rule out a consecutive photoinduced electron transfer (ConPET) process wherein the photocatalyst radical anion is excited by a second photon to generate the excited-state radical anion *CF_3-4-CzIPN$^{\bullet-}$.[45–48]

Taken together, these results are consistent with the proposed catalytic cycle in Figure 6. The reaction is initiated by an off-cycle reductive quenching of *CF_3-4-CzIPN to generate its ground-state radical anion, which subsequently reduces the HAT reagent followed by mesolytic fragmentation to generate the active amidyl radical species. Alternatively, under the standard reaction conditions, we observe minimal (~2%) formation of a HAT reagent byproduct indicative of homolytic N–O bond cleavage (see Supporting Information for details of experiments characterizing this byproduct), which could also initiate the catalytic cycle upon HAT of the C–H substrate. Experiments are currently ongoing to distinguish between these two possibilities. In subsequent turns of the catalytic cycle, the excited-state photocatalyst oxidizes the benzylic radical intermediate, turning over the cycle to PC$^{\bullet-}$ and furnishing a carbocation. Finally, this carbocation is trapped by a nucleophile to afford the desired product.

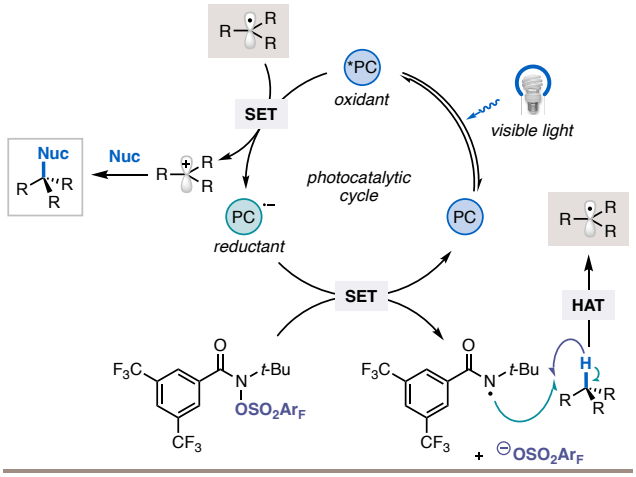

Figure 6. Proposed mechanism for HAT-ORPC amination through a reductive photocatalytic quenching cycle.

CONCLUSION

We have developed a mild, photocatalytic method for site-selective C(sp^3)–H (sulfonyl)amidation, azolation, hydroxylation, esterification, etherification, and halogenation. The method employs readily available, low-cost nucleophiles as coupling partners, an amidyl radical HAT reagent, and a novel organic photocatalyst for HAT-ORPC. Mapping of secondary benzylic C(sp^3)–H substrate chemical space demonstrates the broad scope of the method. Moreover, we show that this HAT-ORPC platform is capable of functionalizing primary benzylic C(sp^3)–H substrates, offering complementary reactivity compared to previous C(sp^3)–H amination methods. Mechanistic studies that include stoichiometric reactions, Stern-Volmer luminescence experiments, and paramagnetic NMR and EPR studies, are consistent with amidyl radical-mediated HAT and suggest that reductive quenching of the CF_3-4-CzIPN photocatalyst is operative. These studies highlight the synthetic opportunities that can accompany further reagent and photocatalyst design in the field.

ASSOCIATED CONTENT

Supporting Information

The Supporting Information is available free of charge on the ACS Publications website.

Experimental procedures, experimental data, C–H substrate chemical space construction, characterization, and spectral data (PDF)
List of SMILES for chemical space (TXT)

Accession Codes

CCDC 2258612, 2258613, and 2258614 contain the supplementary crystallographic data for this paper. These data can be obtained free of charge via www.ccdc.cam.ac.uk/data_request/cif, or by emailing data_request@ccdc.cam.ac.uk, or by contacting The Cambridge Crystallographic Data Centre, 12 Union Road, Cambridge CB2 1EZ, UK; fax: +44 1223 336033.

AUTHOR INFORMATION

Corresponding Author

*Abigail G. Doyle — *Department of Chemistry and Biochemistry, University of California-Los Angeles, Los Angeles, CA 90095, United States;* orcid.ord/0000-0002-6641-0833; Email: agdoyle@chem.ucla.edu

Authors

Madeline E. Ruos — *Department of Chemistry and Biochemistry, University of California, Los Angeles, Los Angeles, California 90095, United States;* orcid.org/0009-0007-6955-8642

R. Garrison Kinney — *Department of Chemistry, Princeton University, Princeton, New Jersey 08544, United States; Department of Chemistry and Biochemistry, University of California, Los Angeles, Los Angeles, California 90095, United States;* orcid.org/0000-0002-1699-5028

Oliver T. Ring — *Early Chemical Development, Pharmaceutical Sciences, Biopharmaceuticals R&D, AstraZeneca Gothenburg, SE-431 83 Mölndal, Sweden; Department of Chemistry and Biochemistry, University of California, Los Angeles, Los Angeles, California 90095, United States;* orcid.org/0000-0003-1984-8688

Present Addresses

†1400 McKean Rd., Spring House, Pennsylvania 19477, United States

Author Contributions

‡M.E.R and R.G.K. contributed equally.

Notes

The authors declare no competing financial interest.

ACKNOWLEDGMENTS

The authors thank Dr. Saeed Kahn, Dr. Samuel Newman-Stonebraker, and Judah Raab for assistance with X-ray crystal structure determinations, Dr. Ta-Chung Ong and Dr. Robert Taylor for assistance with NMR experiments, Judah Raab for assistance with EPR experiments, and Dr. Andrzej Żurański for assistance with DFT calculations. The authors would also like to thank Dr. Staffan Karlsson for assistance with photoflow chemistry scale-up and Dr. Tove Slagbrand for assistance with High-Throughput-Experimentation. This program has been funded through the generous contributions of the National Science Foundation (CHE-1565983) and AstraZeneca. These studies were supported by shared instrumentation grants from the National Science Foundation (CHE-1048804 & NSF-MRI award 2117480) and the NIH Office of Research Infrastructure Programs (S10OD028644).

ABBREVIATIONS

NFSI, *N*-Fluorobenzenesulfonimide; DDQ, 2,3-Dichloro-5,6-dicyano-1,4-benzoquinone.

REFERENCES

(1) For recent reviews, see: (a) Zhang, Z.; Chen, P.; Liu, G. Copper-Catalyzed Radical Relay in C(sp^3)–H Functionalization. *Chem. Soc. Rev.* **2022**, *51* (5), 1640–1658. (b) Golden, D. L.; Suh, S.-E.; Stahl, S. S. Radical C(sp^3)–H Functionalization and Cross-Coupling Reactions. *Nat. Rev. Chem.* **2022**, *6* (6), 405–427. (c) Wang, F.; Chen, P.; Liu, G. Copper-Catalyzed Radical Relay for Asymmetric Radical Transformations. *Accounts Chem. Res.* **2018**, *51* (9), 2036–2046.

(2) Roughley, S. D.; Jordan, A. M. The Medicinal Chemist's Toolbox: An Analysis of Reactions Used in the Pursuit of Drug Candidates. *J. Med. Chem.* **2011**, *54* (10), 3451–3479.

(3) (a) Ritter, J. J.; Minieri, P. P. A New Reaction of Nitriles. I. Amides from Alkenes and Mononitriles 1. *J. Am. Chem. Soc.* **1948**, *70* (12), 4045–4048. (b) Ritter, J. J.; Kalish, J. A New Reaction of Nitriles. II. Synthesis of t-Carbinamines. *J. Am. Chem. Soc.* **1948**, *70* (12), 4048–4050. (c) Sakaguchi, S.; Hirabayashi, T.; Ishii, Y. First Ritter-Type Reaction of Alkylbenzenes Using N-Hydroxyphthalimide as a Key Catalyst. *Chem. Commun.* **2002**, *0* (5), 516–517. (d) Nair, V.; Suja, T. D.; Mohanan, K. A Convenient Protocol for C–H Oxidation Mediated by an Azido Radical Culminating in Ritter-Type Amidation. *Tetrahedron Lett.* **2005**, *46* (18), 3217–3219. (e) Zhang, Y.; Dong, J.; Liu, L.; Liu, L.; Zhou, Y.; Yin, S.-F. Manganese(III) Acetate Catalyzed Oxidative Amination of Benzylic C(sp^3)–H Bonds with Nitriles. *Org. Biomol. Chem.* **2017**, *15* (14), 2897–2901. (f) Michaudel, Q.; Thevenet, D.; Baran, P. S. Intermolecular Ritter-Type C–H Amination of Unactivated sp^3 Carbons. *J. Am. Chem. Soc.* **2012**, *134* (5), 2547–2550. (g) Kiyokawa, K.; Takemoto, K.; Minakata, S. Ritter-Type Amination of C–H Bonds at Tertiary Carbon Centers Using Iodic Acid as an Oxidant. *Chem. Commun.* **2016**, *52* (89), 13082–13085. (h) Li, G.-X.; Morales-Rivera, C. A.; Gao, F.; Wang, Y.; He, G.; Liu, P.; Chen, G. A Unified Photoredox-Catalysis Strategy for C(sp^3)–H Hydroxylation and Amidation Using Hypervalent Iodine. *Chem. Sci.* **2017**, *8* (10), 7180–7185. (i) Duhamel, T.; Martínez, M. D.; Sideri, I. K.; Muñiz, K. 1,3-Diamine Formation from an Interrupted Hofmann–Löffler Reaction: Iodine Catalyst Turnover through Ritter-Type Amination. *ACS Catal.* **2019**, *9* (9), 7741–7745.

(4) Shen, T.; Lambert, T. H. C–H Amination via Electrophotocatalytic Ritter-Type Reaction. *J. Am. Chem. Soc.* **2021**, *143* (23), 8597–8602.

(5) Narobe, R.; Murugesan, K.; Haag, C.; Schirmer, T. E.; König, B. C(sp^3)–H Ritter Amination by Excitation of in Situ Generated Iodine(III)–BF_3 Complexes. *Chem. Commun.* **2022**, *58*, 8778–8781.

(6) For selected examples and reviews, see: (a) Andrus, M. B.; Lashley, J. C. Copper catalyzed allylic oxidation with peresters. *Tetrahedron*. **2002**, *58*(5), 845–866. (b) Eames, J.; Watkinson, M. Catalytic Allylic Oxidation of Alkenes Using an Asymmetric Kharasch–Sosnovsky Reaction. *Angew. Chem. Int. Ed.* **2001**, 40 (19), 3567–3571. (c) *Comprehensive Asymmetric Catalysis*; Jacobsen, E. N., Pfaltz, A., Yamamoto, H., Eds.; Springer: Berlin, 1999; Vol. I-III.

(7) Tran, B. L.; Li, B.; Driess, M.; Hartwig, J. F. Copper-Catalyzed Intermolecular Amidation and Imidation of Unactivated Alkanes. *J. Am. Chem. Soc.* **2014**, *136* (6), 2555–2563.

(8) Suh, S.-E.; Nkulu, L. E.; Lin, S.; Krska, S. W.; Stahl, S. S. Benzylic C–H Isocyanation/Amine Coupling Sequence Enabling High-Throughput Synthesis of Pharmaceutically Relevant Ureas. *Chem. Sci.* **2021**, *12* (30), 10380–10387.

(9) Liu, S.; Achou, R.; Boulanger, C.; Pawar, G.; Kumar, N.; Lusseau, J.; Robert, F.; Landais, Y. Copper-Catalyzed Oxidative Benzylic C(sp^3)–H Amination: Direct Synthesis of Benzylic Carbamates. *Chem. Commun.* **2020**, *56* (85), 13013–13016.

(10) Zheng, Y.-W.; Narobe, R.; Donabauer, K.; Yakubov, S.; König, B. Copper(II)-Photocatalyzed N–H Alkylation with Alkanes. *ACS Catal.* **2020**, *10* (15), 8582–8589.

(11) Chen, X.; Lian, Z.; Kramer, S. Enantioselective Intermolecular Radical Amidation and Amination of Benzylic C−H Bonds via Dual Copper and Photocatalysis. *Angew. Chem. Int. Ed.* **2023**, *62* (13), e202217638.

(12) Liu, X.; Zhang, Y.; Wang, L.; Fu, H.; Jiang, Y.; Zhao, Y. General and Efficient Copper-Catalyzed Amidation of Saturated C−H Bonds Using N-Halosuccinimides as the Oxidants. *J. Org. Chem.* **2008**, *73* (16), 6207–6212.

(13) Dai, L.; Chen, Y.-Y.; Xiao, L.-J.; Zhou, Q.-L. Intermolecular Enantioselective Benzylic C(sp^3)–H Amination by Cationic Copper Catalysis. *Angew. Chem. Int. Ed.* **2023**, e202304427.

(14) Chen, S.-J.; Golden, D. L.; Krska, S. W.; Stahl, S. S. Copper-Catalyzed Cross-Coupling of Benzylic C–H Bonds and Azoles with Controlled N-Site Selectivity. *J. Am. Chem. Soc.* **2021**, *143* (36), 14438–14444.

(15) Bao, X.; Wang, Q.; Zhu, J. Copper-Catalyzed Remote C(sp^3)–H Azidation and Oxidative Trifluoromethylation of Benzohydrazides. *Nat. Commun.* **2019**, *10* (1), 769.

(16) Suh, S.-E.; Chen, S.-J.; Mandal, M.; Guzei, I. A.; Cramer, C. J.; Stahl, S. S. Site-Selective Copper-Catalyzed Azidation of Benzylic C–H Bonds. *J. Am. Chem. Soc.* **2020**, *142* (26), 11388–11393.

(17) Chen, Y.; Yang, B.; Li, Q.-Y.; Lin, Y.-M.; Gong, L. Selectfluor-Enabled Photochemical Selective C(sp^3)–H(Sulfonyl)Amidation. *Chem. Commun.* **2022**, *59* (1), 118–121.

(18) Ramesh, D.; Ramulu, U.; Mukkanti, K.; Venkateswarlu, Y. DDQ-Mediated Direct Oxidative Coupling of Amides with Benzylic and Allylic sp^3 C–H Bonds under Metal-Free Conditions. *Tetrahedron Lett.* **2012**, *53* (23), 2904–2908.

(19) Hou, Z.; Liu, D.; Xiong, P.; Lai, X.; Song, J.; Xu, H. Site-Selective Electrochemical Benzylic C−H Amination. *Angew. Chem. Int. Ed.* **2021**, *60* (6), 2943–2947.

(20) Song, C.; Dong, X.; Yi, H.; Chiang, C.-W.; Lei, A. DDQ-Catalyzed Direct C(sp^3)–H Amination of Alkylheteroarenes: Synthesis of Biheteroarenes under Aerobic and Metal-Free Conditions. *ACS Catal.* **2018**, *8* (3), 2195–2199.

(21) Hou, Z.-W.; Li, L.; Wang, L. Organocatalytic Electrochemical Amination of Benzylic C–H Bonds. *Org. Chem. Front.* **2021**, *8* (17), 4700–4705.

(22) Buglioni, L.; Beslać, M.; Noël, T. Dehydrogenative Azolation of Arenes in a Microflow Electrochemical Reactor. *J. Org. Chem.* **2021**, *86* (22), 16195–16203.

(23) Das, M.; Zamani, L.; Bratcher, C.; Musacchio, P. Z. Azolation of Benzylic C–H Bonds via Photoredox-Catalyzed Carbocation Generation. *J. Am. Chem. Soc.* **2023**, *145* (7), 3861–3868.

(24) Leibler, I. N.-M.; Tekle-Smith, M. A.; Doyle, A. G. A General Strategy for C(Sp3)–H Functionalization with Nucleophiles Using Methyl Radical as a Hydrogen Atom Abstractor. *Nat. Commun.* **2021**, *12* (1), 6950.

(25) Zhang, Y.; Fitzpatrick, N. A.; Das, M.; Bedre, I. P.; Yayla, H. G.; Lall, M. S.; Musacchio, P. Z. A Photoredox-Catalyzed Approach for Formal Hydride Abstraction to Enable Csp^3–H Functionalization with Nucleophilic Partners (F, C, O, N, and Br/Cl). *Chem. Catal.* **2022**, *2* (2), 292–308.

(26) Tierney, M. M.; Crespi, S.; Ravelli, D.; Alexanian, E. J. Identifying Amidyl Radicals for Intermolecular C–H Functionalizations. *J. Org. Chem.* **2019**, *84* (20), 12983–12991.

(27) Wu, K.; Wang, L.; Colón-Rodríguez, S.; Flechsig, G.; Wang, T. Amidyl Radical Directed Remote Allylation of Unactivated sp^3 C−H Bonds by Organic Photoredox Catalysis. *Angew. Chem. Int. Ed.* **2019**, *58* (6), 1774–1778.

(28) Chen, H.; Fan, W.; Yuan, X.-A.; Yu, S. Site-Selective Remote C(sp^3)–H Heteroarylation of Amides via Organic Photoredox Catalysis. *Nat. Commun.* **2019**, *10* (1), 4743.

(29) Miller, A. S.; Alexanian, E. J. Heteroarylation of Unactivated C–H Bonds Suitable for Late-Stage Functionalization. *Chem. Sci.* **2022**, *13* (40), 11878–11882.

(30) Fazekas, T. J.; Alty, J. W.; Neidhart, E. K.; Miller, A. S.; Leibfarth, F. A.; Alexanian, E. J. Diversification of Aliphatic C–H Bonds in Small Molecules and Polyolefins through Radical Chain Transfer. *Science* **2022**, *375* (6580), 545–550.

(31) Kavarnos, G. J.; Turro, N. J. Photosensitization by Reversible Electron Transfer: Theories, Experimental Evidence, and Examples. *Chem. Rev.* **1986**, *86* (2), 401–449.

(32) Ruccolo, S.; Qin, Y.; Schnedermann, C.; Nocera, D. G. General Strategy for Improving the Quantum Efficiency of Photoredox Hydroamidation Catalysis. *J. Am. Chem. Soc.* **2018**, *140* (44), 14926–14937.

(33) Šakić, D.; Zipse, H. Radical Stability as a Guideline in C–H Amination Reactions. *Adv. Synth. Catal.* **2016**, *358* (24), 3983–3991.

(34) Qin, Q.; Yu, S. Visible-Light-Promoted Redox Neutral C–H Amidation of Heteroarenes with Hydroxylamine Derivatives. *Org. Lett.* **2014**, *16* (13), 3504–3507.

(35) Ortiz, G. X.; Hemric, B. N.; Wang, Q. Direct and Selective 3-Amidation of Indoles Using Electrophilic N-[(Benzenesulfonyl)Oxy]Amides. *Org. Lett.* **2017**, *19* (6), 1314–1317.

(36) Speckmeier, E.; Fischer, T. G.; Zeitler, K. A Toolbox Approach To Construct Broadly Applicable Metal-Free Catalysts for Photoredox Chemistry: Deliberate Tuning of Redox Potentials and Importance of Halogens in Donor–Acceptor Cyanoarenes. *J. Am. Chem. Soc.* **2018**, *140* (45), 15353–15365.

(37) Romero, N. A.; Nicewicz, D. A. Organic Photoredox Catalysis. *Chem. Rev.* **2016**, *116* (17), 10075–10166.

(38) Yokoyama, M.; Inada, K.; Tsuchiya, Y.; Nakanotani, H.; Adachi, C. Trifluoromethane Modification of Thermally Activated Delayed Fluorescence Molecules for High-Efficiency Blue Organic Light-Emitting Diodes. *Chem. Commun.* **2018**, *54* (59), 8261–8264.

(39) Kariofillis, S. K.; Jiang, S.; Żurański, A. M.; Gandhi, S. S.; Alvarado, J. I. M.; Doyle, A. G. Using Data Science To Guide Aryl Bromide Substrate Scope Analysis in a Ni/Photoredox-Catalyzed Cross-Coupling with Acetals as Alcohol-Derived Radical Sources. *J. Am. Chem. Soc.* **2022**, *144* (2), 1045–1055.

(40) Auto-QChem DB https://autoqchem.org/ (accessed 2022-06-22).

(41) Żurański, A. M.; Wang, J. Y.; Shields, B. J.; Doyle, A. G. Auto-QChem: An Automated Workflow for the Generation and Storage of DFT Calculations for Organic Molecules. *React. Chem. Eng.* 2022.

(42) (a) McInnes, L.; Healy, J.; Melville, J. UMAP: Uniform Manifold Approximation and Projection for Dimension Reduction. 2018-02-09. *arXiv*. https://arxiv.org/abs/1802.03426 (accessed 2022-06-22). (b) McInnes, L.; Healy, J.; Saul, N.; Großberger, L. UMAP: Uniform Manifold Approximation and Projection. *J. Open. Source. Softw.* **2018**, *3*, 861.

(43) Cismesia, M. A.; Yoon, T. P. Characterizing Chain Processes in Visible Light Photoredox Catalysis. *Chem. Sci.* **2015**, *6* (10), 5426–5434.

(44) Sherwood, T. C.; Xiao, H.-Y.; Bhaskar, R. G.; Simmons, E. M.; Zaretsky, S.; Rauch, M. P.; Knowles, R. R.; Dhar, T. G. M. Decarboxylative Intramolecular Arene Alkylation Using N-(Acyloxy)Phthalimides, an Organic Photocatalyst, and Visible Light. *J. Org. Chem.* **2019**, *84* (13), 8360–8379.

(45) Xu, J.; Cao, J.; Wu, X.; Wang, H.; Yang, X.; Tang, X.; Toh, R. W.; Zhou, R.; Yeow, E. K. L.; Wu, J. Unveiling Extreme Photoreduction Potentials of Donor–Acceptor Cyanoarenes to Access Aryl Radicals from Aryl Chlorides. *J. Am. Chem. Soc.* **2021**, *143* (33), 13266–13273.

(46) Chernowsky, C. P.; Chmiel, A. F.; Wickens, Z. K. Electrochemical Activation of Diverse Conventional Photoredox Catalysts Induces Potent Photoreductant Activity. *Angew. Chem. Int. Ed.* **2021**, *60* (39), 21418–21425.

(47) Chmiel, A. F.; Williams, O. P.; Chernowsky, C. P.; Yeung, C. S.; Wickens, Z. K. Non-Innocent Radical Ion Intermediates in Photoredox Catalysis: Parallel Reduction Modes Enable Coupling of Diverse Aryl Chlorides. *J. Am. Chem. Soc.* **2021**, *143* (29), 10882–10889.

(48) Soika, J.; McLaughlin, C.; Neveselý, T.; Daniliuc, C. G.; Molloy, John. J.; Gilmour, R. Organophotocatalytic N–O Bond Cleavage of Weinreb Amides: Mechanism-Guided Evolution of a PET to ConPET Platform. *ACS Catal.* **2022**, *12* (16), 10047–10056.

Insert Table of Contents artwork here